Self-Consistent Field Theories for Polymer Brushes. Lattice Calculations and an Asymptotic Analytical Description

C. M. Wijmans* and J. M. H. M. Scheutjens

Department of Physical and Colloid Chemistry, Wageningen Agricultural University, Dreijenplein 6, 6703 HB Wageningen, The Netherlands

E. B. Zhulina

Institute of Macromolecular Compounds, Russian Academy of Science, St. Petersburg 199004, Russia

Received October 18, 1991; Revised Manuscript Received January 30, 1992

ABSTRACT: In this paper we compare two models for calculating the configuration of grafted polymer chains at a solid-liquid interface. The first model is the self-consistent field (SCF) polymer adsorption theory of Scheutjens and Fleer as extended for end-attached chains. In this approach the equilibrium distribution of the polymer is found by averaging the statistical weights of all possible chain conformations that can be generated on a lattice. The second model is an analytical SCF theory developed independently by Zhulina, Borisov, and Priamitsyn and by Milner, Witten, and Cates which predicts the grafted layer structure in the case of strong chain stretching. A comparison is made between the results of both theories, and the deviations are explained from the assumptions made in the less exact analytical theory.

1. Introduction

Polymer chains that are grafted at one end onto an impenetrable surface form a good model for the analysis of numerous systems, such as sterically stabilized colloidal dispersions, block copolymer surfactants at solid–liquid and liquid–liquid interfaces, solutions and melts of block copolymers under the conditions in which microphases are formed, etc. Theoretical analysis of grafted chain layers was initiated by the pioneering work of Alexander.[1] Using scaling arguments,[1-3] the main features of grafted layers were established, particularly the considerable stretching of overlapping chains perpendicular to the grafting surface. This stretching is greatest for the case of a planar grafted layer, so that the thickness of the layer H is proportional to N for solvents of various strengths. This scaling relationship between the layer thickness and the degree of polymerization suggested the picture of a mainly homogeneous layer of constant concentration and at the periphery of the layer a rapid decrease of concentration.

Further progress in the analytical theory of grafted layers was attained using the self-consistent field (SCF) approach proposed by Semenov.[4] This approach is based on assuming large stretching of the grafted chains with respect to their Gaussian dimension to allow the replacement of the set of conformations of a stretched grafted chain by their "average trajectory" (the so-called Newton or strong-stretching approximation) which significantly simplifies the description of the system. This idea was first applied by Semenov to dense grafted layers (i.e., layers without solvent) and led to a very elegant theory of super structure formation in block copolymer melts under strong segregation conditions.

This SCF approach was generalized and applied to grafted polymer layers immersed in low molecular weight solvents[5,6] and solutions or melts of mobile polymers.[7] Many effects were considered, such as the collapse of the layer due to a decrease of the solvent strength,[8] the polydispersity of grafted and mobile chains,[9] deformational[10] and dynamical[11] behavior of grafted layers, etc.

These investigations led to a different picture of the grafted layer structure. The polymer concentration decreases monotonically on going from the surface to the outside of the layer. Furthermore, the free chain ends are distributed throughout the whole layer. The system parameters such as solvent quality, polydispersity, etc., appear to strongly influence the shapes of the volume fraction profile and the free chain end distribution.

The development of an analytical theory was accompanied by investigations of grafted layers by Monte Carlo simulations[12-15] and numerical calculations using a SCF lattice model.[12,16] In the latter method, the equilibrium concentration profile of the grafted layer is found by accounting for all the possible conformations of the polymer chains that can be generated on a planar lattice. Each conformation is weighted by its Boltzmann probability factor. We emphasize that this approach gives exact results within the mean field and lattice model approximations. No further approximations are needed to find the equilibrium distribution. Typical computation time is on the order of minutes on a desktop workstation. Parameters such as molecular weight, grafting density, and solvent quality can easily be varied, thus enabling the study of the grafted layer structure under various conditions. Therefore, a detailed comparison with analytical predictions is feasible.

The aim of this paper is a systematic comparison of the results obtained by the above-mentioned analytical and numerical SCF methods for a planar layer immersed in either a pure solvent or a solution of mobile polymer. An initial comparison of both approaches for the case of only an athermal solvent[17] was very promising. In this paper we consider a wide range of solvent strengths, including very good (better than athermal) and poor solvents.

The combination of these two different methods for the analysis of grafted layers is useful for several reasons. First, it provides a better understanding of the structural organization of grafted chain layers. Second, it enables us to check the validity of the assumptions made in the analytical theory, particularly the Newton approximation. Furthermore, the establishment of direct relationships between the analytical and the numerical results may stimulate further development of both models and their application to other systems.

In this paper we shall consider the equilibrium characteristics of a free, nondeformed planar layer, and its

0024-9297/92/2225-2657$03.00/0

deformational behavior will be considered elsewhere. In sections 2 and 3, we summarize the main ideas behind the numerical lattice model and analytical SCF theories. Section 4 is devoted to the comparison of the results obtained by both methods.

2. Self-Consistent Field Lattice Model

The homopolymer adsorption theory of Scheutjens and Fleer[18,19] calculates the equilibrium distribution of a polymer–solvent system at an interface by taking into account all possible conformations, each weighted by its Boltzmann probability factor. Cosgrove et al.[12] and Hirz[16] showed that this method can be applied to terminally attached chains by restricting the conformations to those whose first chain segment is in the layer adjacent to the surface. In this section we describe both versions for the case of nonadsorbing polymer segments, that is, where segments and solvent molecules are assumed to have the same affinity for the surface. In this case the polymer tends to avoid the surface to minimize the loss of conformational entropy.

Consider a lattice consisting of M layers, numbered $z/l = 1, 2, ..., M$, where z is the distance from the surface and l the thickness of a layer. Layer 1 is the layer adjacent to the surface and layer M is in the bulk solution. We assume full occupancy of the lattice layers. Each layer consists of L lattice sites, each of which accommodates either a polymer segment or a solvent molecule. A fraction λ_0 of the surface of a lattice site is in contact with other sites in the same layer. Similarly, a fraction λ_1 is in contact with sites in a lower layer and another fraction λ_1 with sites in a higher layer. For a simple cubic lattice, which has been used to derive all the results presented in this paper, $\lambda_0 = {}^2/_3$ and $\lambda_1 = {}^1/_6$. The cubic lattice gives an equal a priori probability to a bond between two segments in any of the four directions parallel to the surface as well as to a bond toward the surface or away from the surface.

Polymer Chains in a Concentration Gradient. We first consider the general case of (nongrafted) polymer chains and solvent molecules distributed over the lattice. The chains are N segments long. Within each lattice layer a mean-field approximation is applied, so we can write the volume fraction profile of segments, $\phi(z)$, and solvent molecule, $1 - \phi(z)$, as functions of z alone. In the bulk solution the polymer concentration is ϕ^b. As mentioned above, we assume that there is no net adsorption energy of the polymer segments with respect to that of the solvent. Nearest-neighbor interactions between polymer segments and solvent are accounted for by the Flory–Huggins interaction parameter χ. Because of the mean-field approximation all interactions within a layer are smeared out. This means that the potential energy $u(z)$ of a polymer segment in layer z relative to that in the bulk is given by

$$u(z)/kT = \chi(\langle 1 - 2\phi(z)\rangle - 1 + 2\phi^b) - \ln [1 - \phi(z)] + \ln [1 - \phi^b] \quad (1)$$

where the angular brackets $\langle\ \rangle$ denote a weighted average over three layers, which accounts for the fraction of contacts that a segment or solvent molecule has with its nearest neighbors in these layers. For example, the average volume fraction of nearest-neighbor segments of a site in layer z is given by

$$\langle\phi(z)\rangle = \lambda_1\phi(z-l) + \lambda_0\phi(z) + \lambda_1\phi(z+l) \quad (2)$$

The segment potential $u(z)$, which corresponds to $-kT \ln (p_i)$ in ref 18, is the derivative of the free energy with respect to the segment concentration in layer z; i.e., it is determined by the change in free energy that takes place upon exchanging a solvent molecule in layer z with a single polymer segment in the bulk. This change is comprised of contributions from the loss of interaction energy, $-\chi\langle\phi(z)\rangle$, which is due to the removal of the solvent molecule from layer z, the gain in energy from interactions of the solvent molecule with the bulk solution, $\chi\phi^b$, the gain in interaction energy due to the insertion of the segment into layer z, $\chi\langle 1 - \phi(z)\rangle$, its loss in interaction energy due to its removal from the bulk, $-\chi(1 - \phi^b)$, and a term for the change in the translational entropy of the solvent molecule, $\ln [1 - \phi(z)] - \ln [1 - \phi^b]$. The translational entropy of the solvent is included in $u(z)$, whereas the entropy of the polymer is accounted for in the conformation statistics which are described below.

We define a segment weighting factor $G(z)$ as

$$G(z) = \exp(-u(z)/kT) \quad (3)$$

which is a Boltzmann factor of the segment potential in layer z. Detached segments (monomers) would have a distribution given by $G(z)$. The intermolecular interactions are included in $u(z)$ within the mean-field approximation, but in a chain the distribution of a segment is also affected by that of all the other segments in the same molecule and may depend on its position in the chain. The connectivity of the segments is accounted for in the end-segment weighting factor $G(z,s)$, defined as the average statistical weight of all conformations of an s-mer of which the last segment is located in layer z and the first segment may be located anywhere in the system. If segment s is in layer z, segment $s - 1$ must be located in one of the layers $z - l$, z, or $z + l$. This means that $G(z,s)$ is proportional to $\langle G(z,s-1)\rangle$, the weighted average of statistical weights of $(s-1)$-mers of which the last segment is in one of the layers $z - l, z$, or $z + l$. The angular brackets denote a similar average as defined by eq 2. Furthermore, segment s in layer z contributes a factor $G(z)$. It is now easily seen that a recurrence relation holds which enables us to calculate $G(z,s)$ for all values of s:

$$G(z,s) = \langle G(z,s-1)\rangle G(z) \quad (4)$$

The sequence is started with $G(z,1) = G(z)$, the statistical weight of a monomer. Thus, $G(z,s)$ is calculated for all $s \leq N$, for a given set of values for $u(z)$. To arrive at our goal of finding an expression for the total segment volume fraction $\phi(s,z)$ of the sth polymer segment in layer z, we realize that the sth segment of a polymer of N segments can be viewed as being simultaneously the end segment of an s-mer and of an $(N + 1 - s)$-mer. This means that the total statistical weight of the chain is given by the joint probability that both end segments of the subchains are on the same site or, because of the mean-field approximation and apart from a factor L, in the same layer. Thus, $\phi(s,z)$ becomes

$$\phi(z,s) = CG(z,s)\, G(z,N-s+1)/G(z) \quad (5)$$

Here, the denominator accounts for the fact that segment s is counted twice (belonging to both chain parts). The normalization constant C can be obtained in two ways. In a closed system the total number n of polymer molecules is fixed and C follows from the boundary condition $n = L\sum_z\phi(z,s)$. This relation is valid for any s, since there are n segments s in the system. If we substitute $\phi(z,s)$ from

eq 5 for $s = 1$ or $s = N$, we obtain

$$C = \frac{n}{L\sum_z G(z,N)} \tag{6}$$

Alternatively, C can be expressed in the bulk concentration ϕ^b, which is especially useful for open systems. In the bulk solution $\phi(z,s)$ must equal ϕ^b/N. Moreover, according to eqs 1–3, in the bulk solution, $u(z)$ is zero and all G's are unity. Thus, from eq 5 it follows that

$$C = \phi^b/N \tag{7}$$

Finally, the total polymer volume fraction in layer z is

$$\phi(z) = \sum_s \phi(z,s) \tag{8}$$

This volume fraction profile, obtained for a given $u(z)$ profile, should be consistent with eq 1 for all values of z. This provides a set of M simultaneous equations in M unknown variables $u(z)$, which may be solved by the numerical method (for free as well as grafted chains) given in Appendix 1.

Grafted Chains. Above, we discussed the general case of polymer chains which may adopt any possible conformation. However, if the chains have one of their ends attached to the surface, the first segment must be in the first layer. Consequently, the generation of chains, using eq 4, must start with $G_g(z,1)$ (where the subscript g denotes grafted) being equal to zero for all $z \neq 1$

$$G_g(z,1) = \begin{cases} G(z) & \text{if } z = 1 \\ 0 & \text{if } z \neq 1 \end{cases} \tag{9}$$

and eq 4 is replaced by

$$G_g(z,s) = \langle G_g(z,s-1)\rangle G(z) \tag{10}$$

Generally, $G_g(z,s) \leq G(z,s)$ and $G_g(z,s)$ is zero for $z > s$. In the chain, segment s is the joint between a grafted chain of s segments and a nongrafted free chain of $N - s + 1$ segments. Equation 4 is still valid for generating the conformations starting from the other end of the chain, i.e., the chain section from segment N down to s. Thus, for grafted chains the equivalent of eq 5 is

$$\phi_g(z,s) = C_g G_g(z,s)\, G(z,N-s+1)/G(z) \tag{11}$$

The total number n_g of grafted polymer chains is fixed by the grafting density $\sigma = n_g/L$ and determines the value of the constant C_g according to eq 6.

Grafted Chains in a Solution of Free Polymer. If the grafted layer is immersed in a solution of free polymer chains of N_f segments, both the volume fraction profile $\phi_g(z)$ of the grafted chains and that of the free chains, $\phi_f(z)$, are calculated from the same potential energy profile $u(z)$. In eq 1 the volume fraction of segments $\phi(z)$ is given by $\phi_g(z) + \phi_f(z)$. To find the volume fractions of the mobile chains, $\phi_f(z)$, eqs 4 and 5 are used, and for the grafted chains eqs 9–11 are used. The normalization constant for the free polymer is determined by the bulk volume fraction ($C_f = \phi_f^b/N_f$) and that of the grafted chains by the grafting density ($C_g = \sigma/\sum_z G_g(z,N)$).

Self-Consistent Field. The volume fraction profiles of grafted and free polymer are now given as a function of the segment potential profile. In turn, the segment potential itself is determined by the volume fraction profile (see eq 1). The problem boils down to finding a potential profile which is consistent with the volume fraction profile that it produces. Mathematically, this is equivalent to solving an implicit set of equations for which a numerical iteration scheme is provided in Appendix 1.

3. Analytical Theory

The analytical SCF theory as developed by Zhulina, Priamitsyn, and Borisov[20] and by Milner, Witten, and Cates[6] predicts the asymptotic behavior of grafted chains as the chain length increases. Here we summarize the main equations, emphasizing the similarities and differences with the lattice model and using the same nomenclature as in the previous section.

Consider a planar layer of long ($N_g \gg 1$) fully flexible polymer chains grafted at one end onto a solid surface with relative surface coverage $\sigma = n_g/L$, where n_g is the total number of chains and L the maximum number of chains that could be grafted onto the same surface (l^2/σ is the surface area per chain, which is called σ in ref 5, and σ/l^2 is the number of grafted chains per unit area, which is called σ by Milner, Witten, and Cates[10]). The chain thickness l (which in this paper is assumed to be equal to the Kuhn segment length) corresponds to the lattice spacing in the model of the previous section. When the grafted chains are strongly stretched with respect to their Gaussian dimension, $R_0 = l\sqrt{N}$, the free energy, A, of the system can be written as

$$\frac{A}{LkT} = \frac{3}{2l^3}\int_0^H \phi_g(z',N)\int_0^{z'} E(z|z',N)\,dz\,dz' + \frac{1}{l}\int_0^H f[\phi(z)]\,dz \tag{12}$$

The first term in this equation represents the contribution from the elastic chain stretching in the layer. It is determined by the function $E(z|z',N) = dz/ds$, which gives the local stretching of a chain at distance z from the surface when its free end is located at $z' > z$, and by the volume fraction profile of free chain ends $\phi_g(z',N)$. For a given free chain end location z', the other segments in the chain are assumed to take the most probable path from the grafting surface to z'. The chain stretching function $E(z|z',N)$ determines the position $z(s)$ of every segment, or, equivalently, $1/E(z|z',N)$ gives the segment density of the chain at z when its free end is at z'. In the lattice model there any many conformations for a chain grafted with one end to the surface and with its other end at some specified location. Each segment except the first one is not specifically located in one layer but has a density distribution given by eq 5. However, the average value of $\tilde{z}(s)$, which follows from the volume fraction profile $\phi(z,s)$ of segment s, is

$$\tilde{z}(s) = \frac{\int_z z\phi(z,s)\,dz}{\int_z \phi(z,s)\,dz} = \sigma^{-1}\int_z z\phi(z,s)\,dz/l \tag{13}$$

Assuming that the most probable path may be approximated by the average path, the chain stretching function $E(z|z',N)$ can now be expressed in lattice model parameters as

$$E(z|z',N) \approx \frac{d\tilde{z}(s)}{ds} = \sigma^{-1}\sum_z z(\phi_g(z,s+1) - \phi_g(z,s-1)) \tag{14}$$

The second term in eq 12 accounts for the free energy of mixing the grafted chains with the other molecules in the system, $f[\phi(z)]$ being the free energy density of mixing and $\phi(z)$ the volume fraction of grafted polymer at height z from the surface.

Taking into account the three additional conditions below, one can derive the equilibrium volume fraction

profile $\phi_g(z)$, the free chain end volume fraction profile $\phi_g(z',N)$, the local chain stretching $E(z|z',N)$, and the thickness H of the grafted layer. The first two conditions are

$$\int_0^{z'} \frac{dz}{E(z|z',N)} = N_g \tag{15}$$

and

$$\int_0^H \phi_g(z)\, dz/l = \sigma N_g \tag{16}$$

and the third one is the relationship between $\phi_g(z)$, $\phi_g(z',N)$, and $E(z|z',N)$ which expresses that the total volume fraction at z is the integral over z' of all contributions by chains ending at z':

$$\phi_g(z) = \int_z^H \frac{\phi_g(z',N)\, dz'}{E(z|z',N)} \tag{17}$$

In ref 20 the derivation is carried out by minimizing the free energy function A of eq 12 under these constraints, using Lagrange's method of undetermined multipliers. This results in an expression for $E(z|z',N)$ that does not depend on the character of the interactions in the layer and is given by

$$E(z|z',N) = \frac{\pi}{2N_g}(z'^2 - z^2)^{1/2} \text{ (for } 0 \le z \le H) \tag{18}$$

The chains are stretched inhomogeneously; that is, their stretching is greatest near the grafting surface and zero at the free chain end. The volume fraction profile $\phi(z)$ follows from the potential field $u(z)$, which is given by the equation

$$u(z)/kT = \frac{\delta f[\phi(z)]}{\delta \phi(z)} = \begin{cases} \Lambda - \dfrac{3\pi^2 z^2}{8N_g^2 l^2} & \text{if } 0 \le z \le H \\ 0 & \text{if } z > H \end{cases} \tag{19}$$

where the numerical constant Λ is a Lagrange multiplier defining the reference potential of $u(z)$. If we give Λ a value such that the potential is zero in the bulk, then eq 19 defines the potential analogously to eq 1. The shape of the potential profile $u(z)$ is parabolic and a function only of Nl, the contour length of the chain, but independent of interactions and grafting density. Milner, Witten, and Cates[6] have pointed out the equivalence between following the grafted chain from its free end toward the surface, arriving after a fixed number of segments independent of the position z' of the free end, and following a classical particle in harmonic oscillation which moves from its maximum displacement z' to the center in a time independent of the amplitude z' and with velocity $E(z|z',N)$. In both cases the potential energy profile is parabolic.

The shape of the volume fraction profile is not yet determined once $u(z)$ is found, for it also depends on the exact form of $f[\phi(z)]$. The free energy of mixing can be written as a Flory type of free energy of mixing

$$f[\phi(z)] = [1 - \phi(z)] \ln [1 - \phi(z)] + \chi\phi(z)[1 - \phi(z)] \tag{20}$$

where χ is the Flory–Huggins interaction parameter. The usual contribution of the translational entropy of the polymer chains to the free energy is absent because of the chains being grafted. Substitution of eq 20 into eq 19 gives the following relation between the potential and the volume fraction profile:

$$u(z)/kT = -\ln (1 - \phi(z)) - 2\chi\phi(z) = \begin{cases} \Lambda - \dfrac{3\pi^2 z^2}{8N_g^2 l^2} & \text{if } 0 \le z \le H \\ 0 & \text{if } z > H \end{cases} \tag{21}$$

The expression for $u(z)$ also follows directly from eq 1 by putting $\phi^b = 0$ (all the polymer is grafted so there is no polymer in the bulk) and $\langle\phi(z)\rangle = \phi(z)$. In the analytical approach the difference between the segment site volume fraction and the average volume fraction of nearest-neighbor segments is neglected. Thus, $\langle\phi(z)\rangle = \phi(z) + \lambda_1\{\phi(z+1) - \phi(z)\} - \lambda_1\{\phi(z) - \phi(z-1)\}$ in the analytical theory is

$$\langle\phi(z)\rangle = \phi(z) + \lambda_1 \partial^2\phi(z)/\partial z^2 \tag{22}$$

As we show below in Figure 4, this approximation does not lead to large discrepancies as long as the curvature of the volume fraction profile is small. The value of the numerical constant Λ can be found from the boundary condition at the periphery of the layer. For a Θ-solvent or better than Θ-solvent ($\chi \le 0.5$), $\phi(H) = 0$, while in a worse than Θ-solvent ($\chi > 0.5$), $\phi(H) = \phi'^b$, where ϕ'^b is the equilibrium concentration on the coexistence curve for the limit $N \to \infty$ (see also ref 21). Within the framework of the Flory approximation ϕ'^b is obtained from the condition

$$\Delta\mu_1/kT = \ln (1 - \phi'^b) + \phi'^b + \chi(\phi'^b)^2 = 0 \tag{23}$$

where $\Delta\mu_1$ is the chemical potential of the solvent molecules in the concentrated phase with respect to that in the dilute phase which is pure solvent. Introducing the reduced coordinate $t = z/H$ and average volume fraction $\bar{\phi}$ of polymer in the grafted layer

$$\bar{\phi} = \int_0^1 \phi(t)\, dt = N_g\sigma l/H \tag{24}$$

we obtain the final equation for the profile $\phi(z)$

$$-\ln\left(\frac{1-\phi(t)}{1-\phi'^b}\right) - 2\chi(\phi(t) - \phi'^b) = \frac{3\pi^2\sigma^2(1-t^2)}{8\bar{\phi}^2} \quad \text{if } 0 \le t \le 1$$

$$\phi(t) = 0 \quad \text{if } t > 1 \tag{25}$$

where $\phi'^b = 0$ for $\chi \le 0.5$ and ϕ'^b is given by eq 23 for $\chi \ge 0.5$. The left-hand side of eq 25 is just the expression for $u(z)$ when $\phi^b = \phi'^b$ (assuming $\langle\phi(z)\rangle = \phi(z)$). When $\phi'^b = 0$, eq 25 reduces to eq 21. For worse than Θ-solvents the volume fraction profile drops from $\phi(z) = \phi'^b$ to $\phi(z) = 0$ at the periphery of the layer. This is accompanied by a discontinuity in the segment potential at this point which corresponds to the difference between the segment potential in a solution of concentration ϕ'^b (i.e., $\ln (1 - \phi'^b) + 2\chi\phi'^b$; see eq 21) and that in the bulk of pure solvent (i.e., zero).

In Appendix 2 a simple numerical method is given by which $\phi(t)$ can be obtained from eq 25 for a given combination of χ and σ.

Finally, the free chain end volume fraction profile $\phi_g(z',N)$ is obtained by inversion of the integral relationship in eq 17, where the functions $E(z|z',N)$ and $\phi_g(z)$ are given by eqs 18 and 25, respectively.

Virial Expansion. For low grafting densities ($\phi(t) \ll 1$) the logarithm of eq 20 can be expanded with retention of terms of order ϕ^2 and ϕ^3 to express the free energy function $f[\phi(z)]$ in terms of the virial coefficients $v = 0.5$

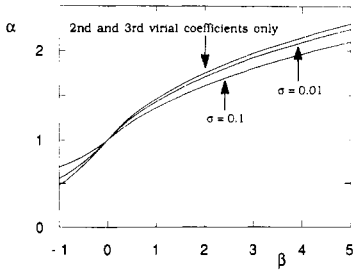

Figure 1. Swelling coefficient α versus the volume interaction parameter β according to eq 31, based on a truncated virial expansion, and as calculated from the more exact eq 25 for grafting densities $\sigma = 0.1$ and 0.01.

$-\chi$ and $w = {}^1/_6$:

$$f[\phi(z)] \approx v\phi^2(z) + w\phi^3(z) \tag{26}$$

This approximation leads to less precise results, but it enables us to find relatively simple expressions for various grafted layer characteristics.[5] Expanding eqs 23 and 25 to powers of $\phi(t)$ gives the corresponding equations for the profiles $\phi(t)$ and coexistence concentration $\phi'^b = -v/2w$. For the particular cases of an athermal and a Θ-solvent the profiles are given by

$$\phi(t)/\bar{\phi} = \begin{cases} \frac{3}{2}(1-t^2) & \text{if } 0 \le t \le 1 \text{ and } \chi = 0 \\ \frac{4}{\pi}(1-t^2)^{1/2} & \text{if } 0 \le t \le 1 \text{ and } \chi = 0.5 \\ 0 & \text{if } t > 1 \end{cases} \tag{27}$$

The corresponding thicknesses of the layer are

$$H = \begin{cases} \left(\frac{8v\sigma}{\pi^2}\right)^{1/3} N_g l & \text{if } \chi = 0 \\ \frac{4}{\pi}\left(\frac{w\sigma^2}{2}\right)^{1/4} N_g l & \text{if } \chi = 0.5 \end{cases} \tag{28}$$

The inversion of the integral relationship in eq 17 gives the following expressions for the free chain end volume fraction profile $\phi_g(t,N)$:

$$\phi_g(t,N) = \begin{cases} 3\sigma t(1-t^2)^{1/2} & \text{if } 0 \le t \le 1 \text{ and } \chi = 0 \\ 2\sigma t & \text{if } 0 \le t \le 1 \text{ and } \chi = 0.5 \\ 0 & \text{if } t > 1 \end{cases} \tag{29}$$

In ref 5 it was shown that for low grafting densities the swelling coefficient α of the layer, defined as $\alpha = H(\chi{=}0)/H(\chi{=}0.5)$, is a universal function of the parameter

$$\beta = \frac{v}{3}(2w^3\sigma^2)^{-1/4} \tag{30}$$

independent of the molecular weight of the grafted chains. The parameter β depends both on the solvent strength and on the grafting density. The relationship between α and β is given by

$$\frac{\pi}{2\beta^2} = \begin{cases} -\frac{\alpha}{\beta} + \left(1 + \frac{\alpha^2}{\beta^2}\right)\arctan\left(\frac{\alpha}{\beta}\right) & \chi \le 0.5 \\ -\frac{5\alpha}{2\beta} + \left(\frac{1}{4} + \frac{\alpha^2}{\beta^2}\right)\arctan\left(\frac{2\alpha}{\beta}\right) & \chi > 0.5 \end{cases} \tag{31}$$

In Figure 1 the function $\alpha(\beta)$ is plotted as given by eq 31. The curve passes through the point (0,1) at the Θ-temperature, where $\beta = 0$ (since $v = 0$) and $\alpha = 1$ by definition. As expected, in worse than Θ-solvents ($\beta < 0$) the swelling coefficient α is smaller than unity, while in good solvents ($\beta > 0$) the polymer layer is thicker than in a Θ-solvent. In most cases the swelling deviates by less than a factor of 2 from that in a Θ-solvent. For comparison, Figure 1 also shows the curves for grafting densities $\sigma = 0.01$ and $\sigma = 0.1$ that have been calculated directly from eq 25 without using the virial expansion. In the first curve only pair and ternary interactions are taken into account; in the latter two curves all higher order interactions are also accounted for. For high grafting densities these higher order interactions, which oppose the variation in swelling, become more important. For $\sigma = 0.1$ the approximation of $\alpha(\beta)$ given by eq 31 is much worse than that for $\sigma = 0.01$. Clearly, eqs 26–31 lose validity for high grafting densities. In the next section we present and compare results from the lattice model and from the analytical theory using the full expression for $f[\phi(z)]$.

Grafted Chains in a Polymer Solution. To conclude this section, we briefly summarize the results for a grafted layer immersed in a solution of short mobile polymer chains with a degree of polymerization $N_f \ll N_g$ and a volume fraction profile denoted by $\phi_f(z)$. Now, the free energy of mixing depends on both profiles, $\phi_g(z)$ and $\phi_f(z)$. Instead of eq 19 we have two simultaneous equations:

$$\frac{\delta f[\phi_g(t),\phi_f(t)]}{\delta\phi_g(t)} = \Lambda_g - K^2t^2 \tag{32}$$

and

$$\frac{\delta f[\phi_g(t),\phi_f(t)]}{\delta\phi_f(t)} = \Lambda_f \tag{33}$$

with

$$K^2 = \frac{3}{8}\left(\frac{\pi H}{N_g l}\right)^2 \tag{34}$$

The numerical constants Λ_g and Λ_f are obtained from the boundary conditions. For the simplest case of grafted and mobile polymers of the same monomer type in an athermal solvent

$$f[\phi_g(t),\phi_f(t)] = \frac{\phi_f(t)}{N_f}\ln[\phi_f(t)] + [1-\phi_f(t)-\phi_g(t)] \times \ln[1-\phi_f(t)-\phi_g(t)] \tag{35}$$

With the boundary conditions $\phi_g(H) = 0$ and $\phi_f(H) = \phi_f^b$ (where ϕ_f^b is the bulk concentration of the mobile polymer) the solution of eqs 32 and 33 is

$$\phi_g(t) = \begin{cases} (1-\phi_f^b)[1-\exp\{-K^2(1-t^2)\}] + \\ \quad \phi_f^b[1-\exp\{-K^2(1-t^2)N_f\}] & \text{if } 0 \le t \le 1 \\ 0 & \text{if } t > 1 \end{cases} \tag{36}$$

$$\phi_f(t) = \begin{cases} \phi_f^b \exp\{-K^2(1-t^2)N_f\} & \text{if } 0 \le t \le 1 \\ \phi_f^b & \text{if } t > 1 \end{cases} \tag{37}$$

No simple algebraic expression for H is available. However, the layer height is completely determined by eqs 34 and 36 and can easily be found numerically from the equation $\bar{\phi} - \int_{t=0}^{1}\phi(t)\,dt = 0$ for given values of ϕ_f^b, N_g, and N_f. The volume fraction profile $\phi_g(z',N)$ of free ends of the grafted chains is given by the equation

$$\phi_g(t,N) = \frac{2Kt}{N_g}\{(1-\phi_f^b)D((K^2(1-t^2))^{1/2}) + \phi_f^b(N_f)^{1/2}D((K^2(1-t^2)N_f)^{1/2})\} \tag{38}$$

where

$$D(y) = e^{-y^2}\int_0^y e^{x^2}\,dx$$

is the Dawson integral.

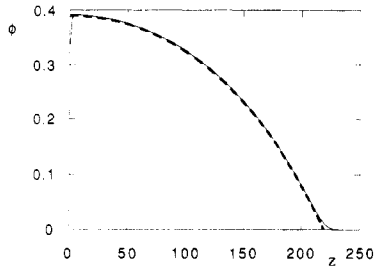

Figure 2. Volume fraction profile $\phi(z)$ according to the analytical theory (dashed curve) and the lattice model (solid curve). Parameters: $N_g = 600$, $\sigma = 0.1$, $\chi = 0$.

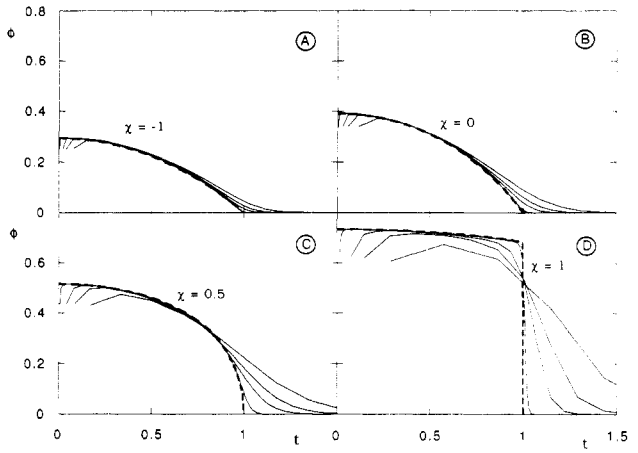

Figure 3. Volume fraction ϕ versus reduced height $t = z/H$ according to the analytical theory (dashed curve) and the lattice model for $N_g = 600$, 100, 50, and 25 (solid curves, in order of increasing deviation from the dashed curve): (A) $\chi = -1$, (B) $\chi = 0$, (C) $\chi = 0.5$, (D) $\chi = 1$. The grafting density σ is 0.1.

4. Comparison of Results from the Two Theories

In all the figures of this section the solid curves represent results obtained by the lattice model while the dashed curves show the asymptotic predictions of the analytical theory. The analytical profiles have been calculated by solving eq 25 for given values of σ and χ.

Figure 2 shows the volume fraction profile of a grafted polymer of 600 segments in an athermal solvent. The grafting density is 0.1; i.e., a polymer chain emerges from 10% of the surface sites. The very good agreement between the analytical predictions and the lattice calculations is striking. Only very close to the grafting surface and at the outer boundary of the grafted layer does a small difference between both curves occur. The lattice calculation shows a depletion zone at the grafting surface. Such a zone was previously seen in Monte Carlo simulations[12,13] and has also been observed by neutron scattering experiments.[22] The presence of the grafting surface restricts the conformational freedom of the polymer. This effect is neglected in the analytical theory. At the other side of the polymer layer the lattice calculation shows a "foot" protruding into the solution whereas the analytical theory predicts that the slope of the profile becomes monotonically steeper with increasing distance. This foot is an exponential decay of the segment density profile, caused by the fact that fluctuations of the average trajectory are large near the chain end where the chain stretching is weak.[23,24]

Figure 3 shows volume fraction profiles for different molecular weights of grafted polymer in a very good solvent ($\chi = -1$; Figure 3A), an athermal solvent (Figure 3B), a Θ-solvent (Figure 3C), and a bad solvent ($\chi = 1$; Figure 3D). In all cases the same (high) grafting density of $\sigma = 0.1$ has been used. The volume fractions are plotted as a function of the reduced height $t = z/H$, where the layer height H is taken from the analytical theory, using only eqs 24 and 25. This enables the comparison of profiles for different chain lengths N_g under the same conditions.

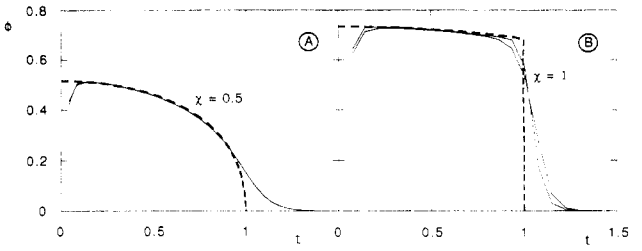

Figure 4. Effect of neglecting the curvature of the segment density profile when calculating the nearest-neighbor interactions. The segment density profiles of C ($\chi = 0.5$) and D ($\chi = 1$) of Figure 3 for $N_g = 100$ are reproduced in graphs A and B, respectively, and a second solid curve in each graph represents the result when in the lattice calculations $\langle 1 - 2\phi(z) \rangle$ in eq 1 is replaced by $1 - 2\phi(z)$. In A the two solid curves virtually coincide. In B the latter curve is slightly more in agreement with the analytical prediction (dashed curve) where the same approximation is made.

According to the analytical theory, $\phi(t)$ is independent of N_g. However, in agreement with Monte Carlo simulations,[13] Figure 3 shows that this is not valid for short chains. The shorter the chain length, the more the lattice model deviates from the analytical theory. Here the effect of the assumption made in the theoretical derivations that $N \gg 1$ is expressed. For all solvent strengths an increase in the chain length leads to a better agreement between both approaches. For a given chain length, increasing the solvent quality also leads to a better agreement. In a better solvent, the grafted layer is more strongly stretched. In a poorer solvent the layer is more dense, so that the unfavorable interactions between polymer segments and solvent molecules are reduced. In other words, the Newton approximation, which assumes strong stretching, is more valid in the case of a good solvent than for a poor solvent. Following parts A–D of Figure 3 for a fixed chain length, the breakdown of the Newton approximation becomes apparent. The deviation is largest in Figure 3D, for $\chi = 1$, where the analytical theory predicts a drop in the segment density profile at $t = 1$, whereas the lattice calculations reveal a more gradual decrease in segment density, especially for the short chains. However, in all cases the analytical theory seems to predict the asymptotic behavior for $N \to \infty$ exactly. It is also worth noting that recent data from neutron scattering experiments on a grafted layer in a bad solvent are well described using a step function for the segment density profile.[25]

There is another effect which contributes to the deviations, especially in poor solvents. In the analytical theory it is assumed that the volume fraction $\phi(z)$ of the segments at position z is the same as $\langle \phi(z) \rangle$, the average volume fraction of their nearest neighbors, whereas in the lattice model these quantities are distinguished; see eq 2. For weak curvatures of the volume fraction profile (good solvent, large N_g) the difference between $\phi(z)$ and $\langle \phi(z) \rangle$ is not great, as $\phi(z-l) + \phi(z+l) \approx 2\phi(z)$, but for strong curvatures a more significant effect on the results is to be expected. This effect can be quantified by introducing the same assumption into the lattice model. This means replacing $\langle 1 - 2\phi(z) \rangle$ by $1 - 2\phi(z)$ in eq 1 for the potential $u(z)$. Parts A and B of Figure 4 give the profiles of parts C and D of Figure 3 for $N = 100$, together with the results for the case that $\langle \phi(z) \rangle$ is set equal to $\phi(z)$. For the Θ-solvent (Figure 4A) the two (solid) curves are virtually the same. For the bad solvent ($\chi = 1$; Figure 4B) the more

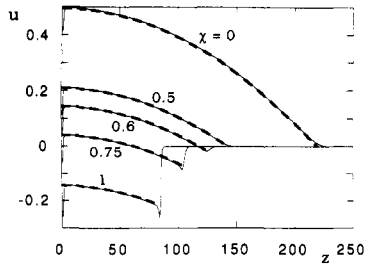

Figure 5. Segment potential energy profiles $u(z)$ for grafted chains of 600 segments and grafting density 0.1 in different solvents: χ = 0, 0.5, 0.6, 0.75, and 1.0 (indicated). Dashed curves: analytical predictions. Solid curves: lattice calculations.

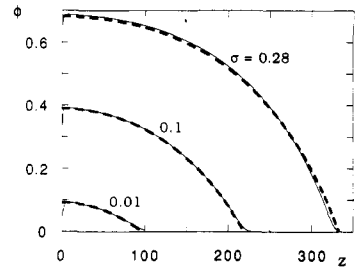

Figure 6. Effect of grafting density σ on the volume fraction profiles $\phi(z)$ according to the analytical theory (dashed curves) and the lattice model (solid curves). Parameters: N_g = 600, χ = 0; σ = 0.01, 0.1, and 0.28 (indicated).

approximate result is in slightly better agreement with the analytical predictions. However, a relatively large deviation still remains, which must be due to the Newton approximation.

Figure 5 shows segment potential energy profiles of a chain of 600 segments in solvents of various strengths (χ = 0, 0.5, 0.6, 0.75, and 1.0). As with the volume fraction profiles, very good agreement is found between predictions from the analytical theory and lattice calculations, except at the grafting surface and at the periphery of the layer. For worse than Θ-solvents the volume fraction profile has a discontinuity at $z = H$. This discontinuity is caused by a jump in the potential profile from $u = -\ln(1-\phi'^b) - 2\chi\phi'^b$ (the value of the potential at the periphery of the grafted layer; see eqs 23 and 25) to $u = 0$ (the bulk solution, in this case pure solvent, being taken as the reference state for the segment potential). As ϕ'^b is the equilibrium volume fraction on the coexistence curve, the chemical potential of the solvent remains constant in the neighborhood of H. The form of the curves is the same in all cases. The curves are shifted in the vertical direction only, reflecting a shift in the reference potential.

Decreasing the grafting density also gives less extended layers as is illustrated in Figure 6, where volume fraction profiles are given for σ = 0.01, 0.1, and 0.28. In all three cases N_g = 600 and χ = 0. Although near the grafting surface and at the outer boundary of the grafted layer the relative deviation between the two theories indeed increases with decreasing σ, the absolute differences remain roughly the same. For σ = 0.28 the lattice model predicts a volume fraction profile that is slightly stronger curved than is predicted by the analytical model. For the limiting case that the grafting denisty is unity the lattice model must give a step function profile (ϕ = 1 for $z \leq N$ and ϕ = 0 for $z > N$). We note that for these long chains a grafting density as high as even 0.1 is not easily reached in real systems. For example, adsorbed block copolymers typically give far lower densities.[26] The grafted amount in equivalent monolayers of segments, σN_g, varies from 168 for σ = 0.28 down to a more reasonable value of 6 for σ = 0.01.

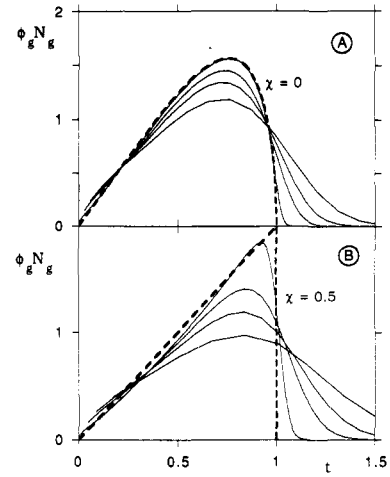

Figure 7. Distribution function of free ends, $\phi_g(t,N)$ N_g, for chains of 600, 100, 50, and 25 segments and grafting density σ = 0.1, according to the analytical theory (dashed curves) and the lattice model (solid curves): (A) in an athermal solvent; (B) in a Θ-solvent.

So far, we have only compared the overall volume fraction profiles predicted by both theories. End-segment distribution profiles are plotted in Figure 7A for an athermal solvent and in Figure 7B for a Θ-solvent. Again, we use the reduced height ($t = z/H$) as the abscissa in order to represent the curves for different chain lengths in one figure. Moreover, we have multiplied $\phi_g(z,N)$ by N_g; i.e., the areas under the curves are all the same. As was the case with the total volume fraction profile, the agreement between the analytical theory and the lattice model becomes better for longer chain lengths. The most striking feature when comparing parts A and B of Figure 7 is the far better agreement for long chains in an athermal solvent compared to a Θ-solvent. However, this is mainly due to a difference in approximation. The results for the athermal solvent have been calculated using eq 38 with $\phi_f^b = 0$. This is an exact expression for $\phi_g(z,N)$ within the strong-stretching limit. Such an expression for Θ-solvents is not available. Therefore, the results for the Θ-solvent were calculated using eq 29, which was derived using the virial expansion of $f[\phi(z)]$. In spite of this approximation, it is clear that we expect a finite end-segment volume fraction throughout the layer, also near the grafting surface, even if the grafting density is high and irrespective of the solvent strength.

We conclude by discussing the case of a grafted polymer layer immersed in an athermal solution of short mobile chains of a chemical nature identical to the grafted polymer. Parts A and B of Figure 8 show volume fraction profiles versus reduced height t for ϕ_f^b = 0.1 and 0.5, respectively, with N_f = 10, σ = 0.1, and different values of N_g. Increasing the bulk volume fraction ϕ_f^b of the mobile chains compresses the grafted layer from H = 67 in Figure 8A to H = 48 in Figure 8B. Just as for grafted layers immersed in pure solvent, longer chain lengths of the grafted polymer give a better agreement between the analytical predictions and the lattice model. It is seen in Figure 8B that the mobile chains are able to penetrate throughout the grafted layer. This is due to their short length in comparison with the grafted polymer. The mobile polymer of the same chain length as the grafted polymer would only penetrate partly into the grafted layer.[27-28]

5. Conclusions

Very good agreement is found between the analytical theory and the lattice calculations. Only at low grafting

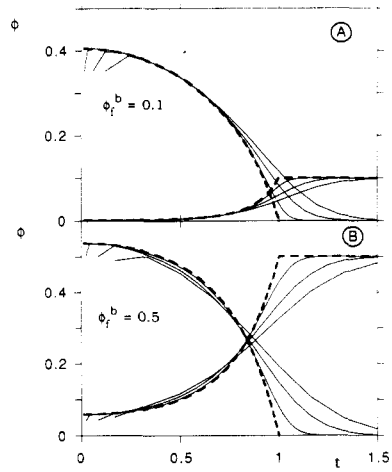

Figure 8. Volume fraction profiles of a grafted layer (N_g = 200, 50, and 25; σ = 0.1) immersed in an athermal solution of short mobile polymers (N_f = 10) of a chemical identical nature. Dashed curves: analytical theory. Solid curves: lattice model. Bulk volume fraction of the mobile polymer: (A) ϕ_f^b = 0.1; (B) ϕ_f^b = 0.5.

densities of short chains in a poor solvent considerable deviations are found between the two approaches because of the breakdown of the Newton approximation (strong chain stretching limit) in the analytical theory. The derivation of elegant expressions for the layer structure by expanding the density of free energy of volume interactions in a virial series, as was done in ref 5, is only valid for relatively low grafting densities (see Figure 1).

Acknowledgment. E.B.Z. acknowledges financial support from the Alexander von Humboldt Foundation and the hospitality of Wageningen Agricultural University. We thank Lawrence Fischel for improving the text.

Appendix 1

Iteration Scheme for the Lattice Model. As we have only one type of segment and one solvent, our iteration scheme can be quite simple (Evers et al. give a general scheme for systems with more than one different segment type). For a given set of values of $u(z)$, $G(z) = \exp(-u(z))$ is calculated and, from these Boltzmann factors, the volume fraction profile of grafted and free polymer is found (using eqs 3–11). The volume fraction, $\phi_s(z)$, of solvent in layer z is obtained from eq A1:

$$\phi_s(z) = (1 - \phi^b) \exp\{-u(z) + \chi(\langle 1 - 2\phi(z)\rangle - 1 + 2\phi^b)\} \tag{A1}$$

Thus, for given values of $u(z)$, the volume fractions of grafted polymer, $\phi_g(z)$, of free polymer, $\phi_f(z)$, and of solvent, $\phi_s(z)$, can be calculated. In each layer z the sum of these volume fractions should obey the boundary constraint:

$$F(z) = \phi_g(z) + \phi_f(z) + \phi_s(z) - 1 = 0 \tag{A2}$$

The objective functions $F(z)$ form a set of M simultaneous equations (one for each layer) in M unknown potentials $u(z)$. This set can be solved by standard numerical methods, e.g., using the Fortran program of Powell.[29]

Computational Aspects for Grafted Chains. For long chains and high grafting densities, i.e., when the chains are strongly stretched, the potentials $u(z)$ are high and $G(z) = \exp(-u(z)/kT)$ is smaller than unity. As $G(z)$ is recursively applied in eqs 4 and 10, the values of $G(z,s)$ and $G_g(z,s)$ become extremely small for large s while the normalization constant $C_g = \sigma/\sum_z G_g(z,N)$ becomes very large, easily exceeding the available numerical range on a computer. Obviously, since the volume fraction of grafted polymer, $\phi_g(z,s)$, is on the order of unity, the product of these quantities must be near unity; see eq 11. The numerical overflow and underflow can be avoided by proper scaling. First, we realize that $G(z,s)$ may be very small at small z and that it is unity for large z, i.e., in the bulk, but that we need only the initial part of the curve because in eq 11 $G(z,s)$ is multiplied by $G_g(z,s)$, which is zero for $z > s$. Consequently, the quantities $G(z,N-s+1)$ for $z > s$ are irrelevant and may be set to zero. This eliminates the largest values and enables a substantial rescaling of the relevant section of $G(z,s)$.

Consider the extreme case of straight chains (when the grafted density $\sigma = 1$). Each segment s would be in layer $z = s$. Mathematically, $\phi_g(z,s) = 1$ if $z = s$ and $\phi_g(z,s) = 0$ if $z \neq s$. Then, the only relevant quantities would be $G(N-s+1,s)$ and $G_g(s,s)$. In the following procedure we normalize the distribution functions so that these most important quantities are of order unity.

Define scaled distribution functions $\tilde{G}(z,s)$ and $\tilde{G}_g(z,s)$ as

$$\tilde{G}(z,s) = \begin{cases} \langle \tilde{G}(z,s-1)\rangle G(z)\, c(s) & \text{if } z \le N - s + 1 \\ 0 & \text{otherwise} \end{cases} \tag{A3}$$

$$\tilde{G}_g(z,s) = \langle \tilde{G}_g(z,s-1)\rangle G(z)\, c_g(s) \tag{A4}$$

where $c(s)$ and $c_g(s)$ are introduced to compensate the low values of $G(z)$ and are chosen so that $\tilde{G}(N-s+1,s)$ and $\tilde{G}_g(s,s)$ remain on the order of unity. For example, set $c(s)$ and $c_g(s)$ equal to unity for $s = 1$ and $c(s) = 1/\tilde{G}(N-s+1,N-s+1)$ and $c_g(s) = 1/\tilde{G}_g(s-1,s-1)$ for $s > 1$. Essentially, eqs A3 and A4 replace eqs 4 and 10, respectively. The relations between the scaled and unscaled quantities are

$$\tilde{G}(z,s) = \begin{cases} G(z,s)\prod_{s'=1}^{s} c(s') & \text{if } z \le N - s + 1 \\ 0 & \text{otherwise} \end{cases} \tag{A5}$$

and

$$\tilde{G}_g(z,s) = G_g(z,s)\prod_{s'=1}^{s} c_g(s') \tag{A6}$$

but the functions $G(z,s)$ and $G_g(z,s)$ are not used. The factors $c(s)$ and $c_g(s)$ are not too far from unity, while the multiple products in eqs A5 and A6 may be very large. The next step is to compute the scaled distribution function $\tilde{\phi}_g(z,s)$ of segment s

$$\tilde{\phi}_g(z,s) = \tilde{G}_g(z,s)\, \tilde{G}(z,N-s+1)/G(z) \tag{A7}$$

and normalize it to obtain $\phi_g(z,s)$

$$\phi_g(z,s) = \frac{\sigma\tilde{\phi}_g(z,s)}{\sum_z \tilde{\phi}_g(z,s)} \tag{A8}$$

This scheme applies only to grafted chains. For free chains the function $G(z,s)$ is especially relevant for large values of z and does not need to be scaled.

Appendix 2

Iteration Scheme for Solving Equation 25. This method consists of a pair of nested loops. In the main iteration loop the variable $\bar{\phi}$ is adjusted until $\bar{\phi} - \int_{t=0}^{1}\phi(t)\, dt < \epsilon$, where ϵ can be chosen as an arbitrarily small number. We have used $\epsilon = 10^{-6}$. The function $\phi(t)$ is obtained in a subiteration which solves $\phi(t)$ for a series of

t values, using eq 25 and the current value of $\bar{\phi}$. From the values of $\phi(t)$ the integral $\int_{t=0}^{1}\phi(t)\,dt$ can be approximated. For example, if $\phi(t)$ is known at $t' = \delta, 3\delta, 5\delta, ..., 1 - \delta$, where δ is a sufficiently small number, the integral is approximately $2\delta\sum_{t'}\phi(t')$. Our results are obtained with $\delta = 10^{-4}$.

References and Notes

(1) Alexander, S. *J. Phys.* (*Paris*) **1977**, *38*, 983.
(2) de Gennes, P.-G. *J. Phys* (*Paris*) **1976**, *37*, 1445.
(3) de Gennes, P.-G. *Macromolecules* **1980**, *13*, 1069.
(4) Semenov, A. N. *Sov. Phys. JETP* **1975**, *61*, 733.
(5) Zhulina, E. B.; Borisov, O. V.; Priamitsyn, V. A. *J. Colloid Interface Sci.* **1990**, *137*, 495.
(6) Milner, S. T.; Witten, T. A.; Cates, M. E. *Macromolecules* **1988**, *21*, 2610.
(7) Zhulina, E. B.; Borisov, O. V.; Brombacher, L. *Macromolecules* **1991**, *24*, 4679.
(8) Zhulina, E. B.; Borisov, O. V.; Priamitsyn, V. A.; Birshtein, T. M. *Macromolecules* **1991**, *24*, 140.
(9) Milner, S. T.; Witten, T. A.; Cates, M. E. *Macromolecules* **1989**, *22*, 853.
(10) Milner, S. T.; Witten, T. A.; Cates, M. E. *Europhys. Lett.* **1988**, *5*, 413.
(11) Klushin, L. I.; Skvortsov, A. M. *Macromolecules* **1991**, *24*, 1549.
(12) Cosgrove, T.; Heath, T.; Van Lent, B.; Leermakers, F.; Scheutjens, J. *Macromolecules* **1987**, *20*, 1692.
(13) Chakrabarti, A.; Toral, R. *Macromolecules* **1990**, *23*, 2016.
(14) Lai, P.-Y.; Binder, K. *J. Chem. Phys.*, in press.
(15) Lai, P.-Y.; Zhulina, E. B., submitted for publication in *J. Phys.* (*Paris*).
(16) Hirz, S. M.Sc. Thesis, University of Minnesota, 1987.
(17) Skvortsov, A. M.; Gorbunov, A. A.; Pavlushkov, I. V.; Zhulina, E. B.; Borisov, O. V.; Priamitsyn, V. A. *Polym. Sci. USSR* **1988**, *30*, 1706.
(18) Scheutjens, J. M. H. M.; Fleer, G. J. *J. Phys. Chem.* **1979**, *83*, 1619.
(19) Scheutjens, J. M. H. M.; Fleer, G. J. *J. Phys. Chem.* **1980**, *84*, 178.
(20) Zhulina, E. B.; Priamitsyn, V. A.; Borisov, O. V. *Polym. Sci. USSR* **1989**, *31*, 205.
(21) Shim, D. F. K.; Cates, M. E. *J. Phys.* (*Paris*) **1989**, *50*, 3535.
(22) Auroy, P.; Auvray, L.; Leger, L. *Phys. Rev. Lett.* **1991**, *66*, 719.
(23) Witten, T. A.; Leibler, L.; Pincus, P. *Macromolecules* **1990**, *23*, 824.
(24) Milner, S. T. *J. Chem. Soc., Faraday Trans.* **1990**, *86*, 1349.
(25) Auroy, P.; Auvray, L.; Leger, L. *Macromolecules* **1991**, *24*, 2523.
(26) Evers, O. A.; Scheutjens, J. M. H. M.; Fleer, G. J. *J. Chem. Soc., Faraday Trans.* **1990**, *86*, 1333.
(27) Van Lent, B.; Israels, R.; Scheutjens, J. M. H. M.; Fleer, G. J. *J. Colloid Interface Sci.* **1990**, *137*, 380.
(28) Ligoure, C.; Leibler, L. *J. Phys.* (*Paris*) **1990**, *51*, 1313.
(29) Powell, M. J. D. In *Numerical Methods for Nonlinear Algebraic Equations*; Rabinowitz, P., Ed.; Gordon and Breach: London, 1970; p 115.